Available online at www.derpharmachemica.com

Scholars Research Library

Der Pharma Chemica, 2010, 2(4): 324-335
(http://derpharmachemica.com/archive.html)

ISSN 0975-413X

Pharmacophore modeling and 3D-QSAR studies on flavonoids as α -glucosidase inhibitors

Vipin Kumar*, Sunil Kumar and Poonam Rani

Institute of Pharmaceutical Sciences,
Kurukshetra University, Kurukshetra, India.

ABSTRACT

Pharmacophore mapping studies were undertaken for a set of 29 flavonoids as α-glucosidase inhibitors. Four point pharmacophores with two hydrogen bond acceptor, one hydrogen bond donor and one aromatic ring as pharmacophoric features were developed. Amongst them the pharmacophore hypothesis AADR1 yielded a statistically significant 3D-QSAR model with 0.903 as R^2 value and was considered to be the best pharmacophore hypothesis. The developed pharmacophore model was externally validated by predicting the activity of test set molecules. The squared predictive correlation coefficient of 0.69 was observed between experimental and predicted activity values of test set molecules. The geometry and features of pharmacophore were expected to be useful for the design of selective α-glucosidase inhibitors.

Keywords: Flavonoids, α-glucosidase, 3D-QSAR, pharmacophore hypothesis, regression coefficient, squared predictive correlation coefficient.

INTRODUCTION

More than 90% of diabetic patient suffers from type-2 diabetes, that is non - insulin dependent diabetes mellitus, which is characterized by insulin resistance and hyperglycemia [1]. Diabetes is a major and growing public health problem throughout the world, with an estimated worldwide prevalence in 2000 of 150 million people, expected to rise up to 220 million people by 2010 [2]. There has been an explosion of introduction of new classes of pharmacologic agents [3] including insulin and insulin analogues [4, 5], sulfonylureas [6], bigunides [7], glitazones (thiazolidinediones) [8, 9], and α -glucosidase inhibitors [10] are one of them.

α- glucosidase belong to the glycosyl hydrolase-31, family of hydrolases and its major function is hydrolysis of terminal, non-reducing 1, 4-linked α-D-glucosidase with release of α -D-glucose. α -glucosidase has drawn a special interest of the pharmaceutical research community because in earlier studies it was shown that the inhibition of its catalytic activity resulted in the retardation of glucose absorption and decrease in postprandial blood glucose level [11]. The α-glucosidase

inhibitors might be a reasonable option as first-line drug in the treatment of patients with diabetes mellitus as it specifically targets postprandial hyperglycaemia. α-glucosidase inhibitors are expected to cause no hypoglycaemic events or other life-threatening events, even at overdoses, and cause no weight gain [12]. Acarbose, an α -glucosidase inhibitor, which delays the absorption of carbohydrate from the small intestine, reduces postprandial hyperglycemia in patients with type 2 diabetes [13].

Flavonoids are widely distributed in plants such as vegetable and fruits. Some of the flavonoids were known to inhibit α -glucosidase enzyme. The primary structure of flavonoids consists of two moieties: benzopyran and phenyl ring groups. The variation in the phenyl ring and the linkage between the benzopyran and phenyl groups are the basis for the classification of flavonoids into six groups: flavones, flavonol, flavonone, isoflavone, flavan-3-ol, and anthocynidin groups [19].

The pharmacophore modeling is a well established approach to quantitatively explore common chemical features among a considerable number of structures and qualified pharmacophore model could also be used as a query for searching chemical databases to find new chemical entities. Pharmacophore modeling correlates activities with the spatial arrangement of various chemical features [14]. Ligand-based drug design approaches like pharmacophore mapping [15] and quantitative structure-activity relationship [16] can be used in drug discovery in several ways, e.g. rationalization of activity trends in molecules under study, prediction of the activity of novel compounds, database search studies in search of new hits and to identify important features for activity [17].

This paper describes the development of a robust ligand-based 3D-pharmacophore hypothesis using pharmacophore alignment and scoring engine PHASE for flavonoids as α-glucosidase inhibitors. The alignment obtained from the pharmacophoric points is used to derive a pharmacophore-based 3D-QSAR model. Such a pharmacophore model provides a rational hypothetical picture of primary chemical features responsible for activity [18].

MATERIALS AND METHODS

Dataset

The in vitro biological data of a series of 29 flavonoids [19] having α-glucosidase inhibitory activity was used for the present studies. The α-glucosidase inhibitory activity was expressed as IC_{50} i.e., concentration in μm required for 50% inhibition of enzyme activity. The dataset was divided randomly into training set and test set by considering the 70% of the total molecules in the training set and 30% in the test set. Twenty one molecules forming the training set were used to generate pharmacophore models and prediction of the activity of test set (08 analogues) molecules was used as a method to validate the proposed models.

Pharmacophore modeling

Pharmacophore modeling and 3-D database searching are now recognized as integral components of lead discovery and lead optimization. The continuing need for improved pharmacophore based tools has driven the development of 'PHASE' (20). To reach our research objectives we have used 'PHASE': a module of Schrödinger's drug design software [21].

Ligand Preparation

The first step for pharmacophore mapping was ligand preparation. The chemical structures of all the compounds were drawn in maestro and geometrically refined using LigPrep module. LigPrep

is a robust collection of tools designed to prepare high quality, all-atom 3D structures for large numbers of drug-like molecules, starting with 2D or 3D structures in SD or Maestro format. The simplest use of LigPrep produces a single, low-energy, 3D structure with correct chiralities for each successfully proposed input structure.

While performing this step, chiralities were determined from 3D structure and original states of ionization were retained. Tautomers were generated using Macro Model method discarding current conformers. The conformations were generated by the Monte Carlo (MCMM) method as implemented in Macro Model version 9.6 using a maximum of 2,000 steps with a distance-dependent dielectric solvent model and an OPLS-2005 force field. All the conformers were subsequently minimized using Truncated Newton Conjugate Gradient (TNCG) minimization up to 500 interactions. For each molecule, a set of conformers with a maximum energy difference of 30 kcal/mol relative to the global energy minimum conformers were retained. The conformational searches were done for aqueous solution using the generalized born/solvent accessible surface (GB/SA) continuum solvation model [22].For molecule 15, 16, 17 the original stereochemistry were maintained.

Creation of Pharmacophoric Sites

The next step in developing a pharmacophore model is to use a set of pharmacophoric features to create pharmacophore sites (site points) for all the ligands. In the present study, an initial analysis revealed that three chemical feature types i.e., hydrogen-bond acceptor (A), hydrogen bond donor (D), and aromatic ring (R) could effectively map all critical chemical features of all molecules in the data set. The minimum and maximum sites for all the features were kept 3 and 4 respectively. These features were selected and used to build a series of hypothesis with find the common pharmacophore option in Phase.

Searching Common Pharmacophore

In this step, pharmacophores from all conformations of the ligands in the training set were examined and those pharmacophores that contain identical sets of features with very similar spatial arrangements were grouped together. If a given group is found to contain at least one pharmacophore from each ligand, then this group gives rise to a common pharmacophore. Any single pharmacophore in the group could ultimately become a common pharmacophore hypothesis. Common pharmacophores are identified using a tree-based partitioning technique that groups together similar pharmacophores according to their inter site distances, i.e., the distances between pairs of sites in the pharmacophore

Scoring Hypothesis

In this step, common pharmacophore hypothesis were examined using a scoring function to yield the best alignment of the active ligands using an overall maximum root mean square deviation (RMSD) value of 1.2 Å for distance tolerance. The quality of alignment was measured by survival score (23).

Generation of 3D-QSAR Model

Phase provides the means to build 3D-QSAR models for a set of ligands that are aligned to a selected hypothesis. The Phase 3D-QSAR model partitions the space occupied by the ligands into a cubic grid. Any structural component can occupy part of one or more cubes. A cube is occupied by a feature if its centroid is within the radius of the feature. We can set the size of the cubes by changing the value in the Grid spacing text box. The regression is done by constructing a series of models with an increasing number of PLS factors. In present case, the pharmacophore

based model was generated by keeping 1Å grid spacing and 3 as maximum number of PLS factors.

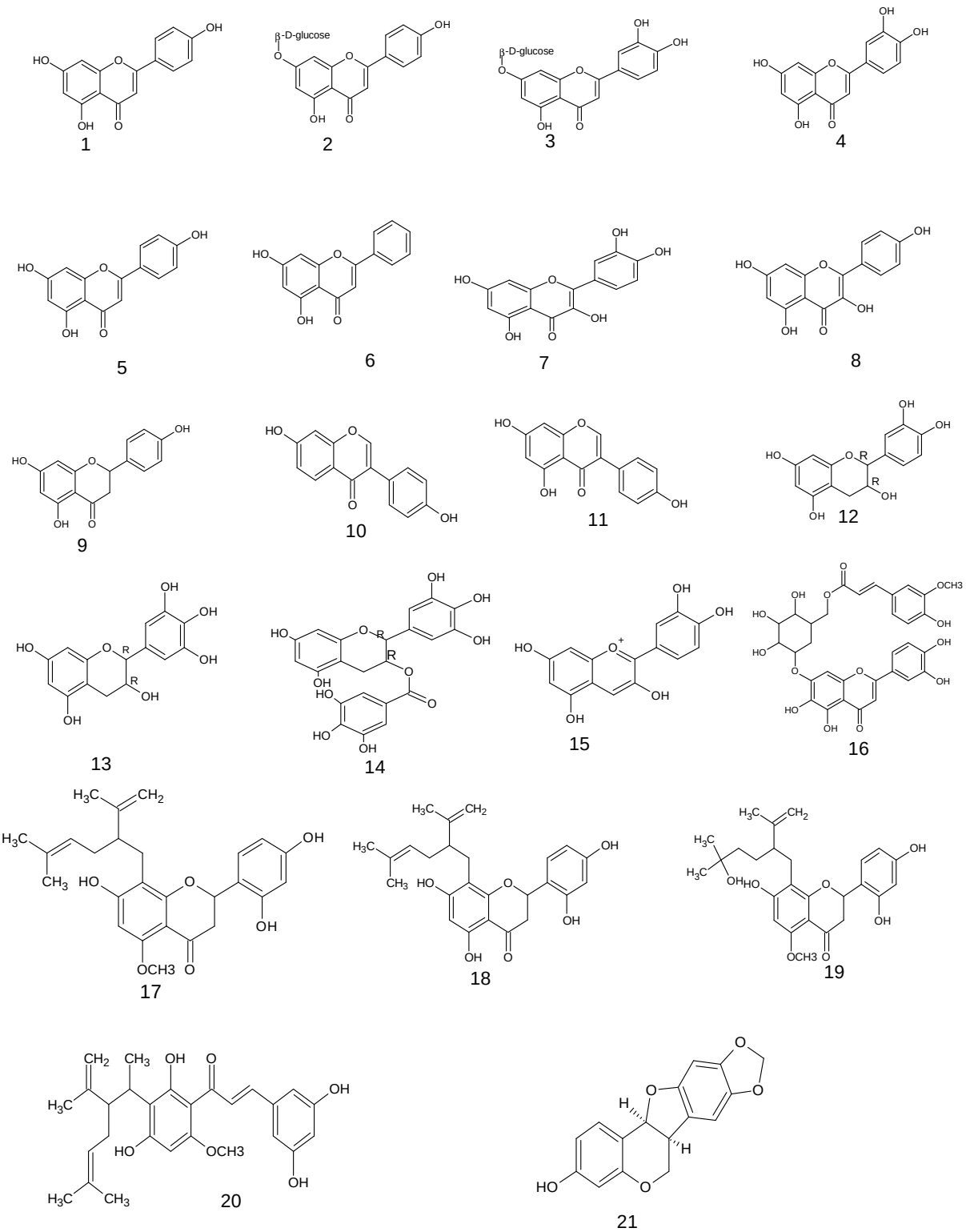

Figure 1: Chemical structure of the 21 training set molecules

Validation of Pharmacophore Model

Validation is a crucial aspect of pharmacophore design, particularly when the model is built for the purpose of predicting activities of molecules in external test series (24). In the present case,

the developed pharmacophore model was validated by predicting the activity of test set molecules. The correlation between the experimental and predicted activities of the test set molecules was determined.

RESULTS AND DISCUSSION

The α-glucosidase inhibitors can retard the liberation of α-D-glucose of oligosaccharides and disaccharides from dietary complex carbohydrates, delay glucose absorption, and, therefore suppress postprandial hyperglycaemia [25]. Such inhibitors, including acarbose and voglibose, are currently used clinically in combination with either diet or other anti-diabetic agents to control blood glucose levels of patients [26]. A main drawback of the current α-glucosidase inhibitors (such as acarbose) is the presence of side effects such as abdominal bacterial fermentation of undigested carbohydrates in the colon [27] To either avoid or decrease the adverse effects of current agents and also to provide more candidates of drug choices, it is still necessary to search for new α-glucosidase inhibitors for further drug development [28]. Some flavonoids from natural sources are studied which possess the α-glucosidase inhibitory activity [19].

Ligand-based drug design relies on knowledge of other molecules that bind to the biological target of interest. These molecules may be used to derive a pharmacophore which defines the minimum necessary structural characteristics a molecule must possess in order to bind to the target [29]. In other words, a model of the biological target is built based on the knowledge of what binds to it and this model in turn may be used to design new molecular entities that interact with the target.

Twenty one molecules forming the training set were used to develop the pharmacophore models. The pharmacophoric features selected for creating sites were hydrogen bond acceptor (A), hydrogen bond donor (D), and aromatic ring (R). Pharmacophore models containing three to four features were generated. The three featured pharmacophore hypotheses were rejected due to low value of survival score, as they were unable to define the complete binding space of the selected molecules. Four featured pharmacophore hypotheses were selected and subjected to stringent scoring function analysis.

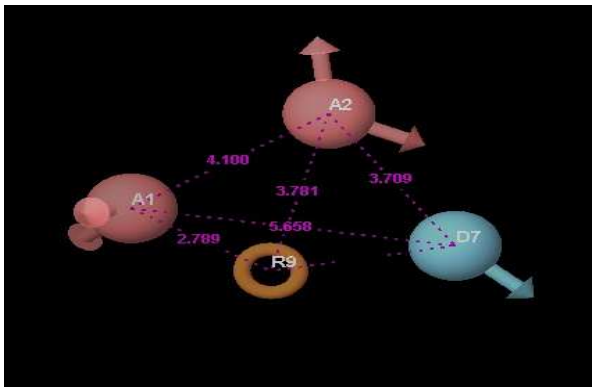

Figure 2: PHASE generated pharmacophore model AADR1 illustrating hydrogen bond acceptor (A1, A2; pink), hydrogen bond donor (D7; blue) and aromatic ring (R9; orange) features with distances (in Å) between different sites of AADR1.

The results of four featured pharmacophore hypotheses, labeled AADR1, AADR2, and AADR3 are presented in Table 1. The first hypothesis AADR1 is the best hypothesis in this study,

characterized by highest survival score (3.084), the best regression coefficient (0.903) and Pearson-R (0.8332). The pharmacophore hypothesis AADR1 is presented in Figure 2. The features represented by this hypothesis are two hydrogen bond acceptor (A), one hydrogen bond donor (D), and one aromatic ring (R). The distances and angles between different sites of AADR1 are given in Table 2 and 3 respectively.

Table 1: Parameters of four featured pharmacophore hypotheses

Sr. No.	Hypothesis	Survival Score	R^2	Pearson-R
1	AADR1	3.084	0.903	0.8332
2	AADR2	3.007	0.814	0.7935
3	AADR3	2.864	0.728	0.7754

Table 2: Distances between different sites of model AADR1

Site-1	Site-2	Distance (Å)	Site-1	Site-2	Distance (Å)
A2	A1	4.100	A1	D7	5.658
A2	D7	3.709	A1	R9	2.789
A2	R9	3.781	D7	R9	3.258

For each ligand, one aligned conformer based on the lowest RMSE of feature atom coordinates from those of the corresponding reference feature was superimposed on AADR1.

Table 3: Angles between different sites of model AADR1

Site 1	Site 2	Site 3	Angle	Site 1	Site 2	Site 3	Angle
A1	A2	D7	92.7	A2	D7	A1	46.4
A1	A2	R9	41.2	A2	D7	R9	65.4
D7	A2	R9	51.9	A1	D7	R9	19.0
A2	A1	D7	40.9	A2	R9	A1	75.5
A2	A1	R9	63.3	A2	R9	D7	63.1
D7	A1	R9	22.4	A1	R9	D7	138.6

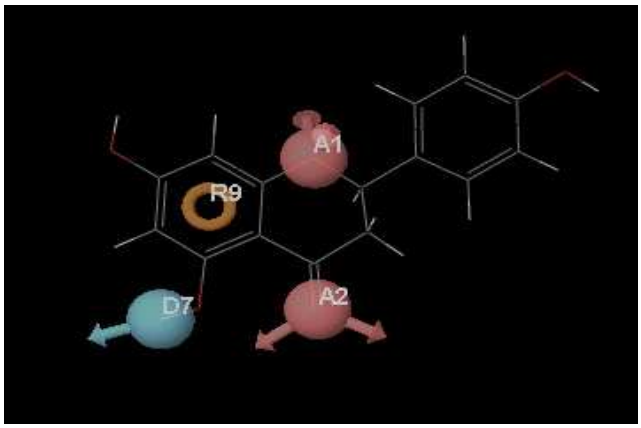

Figure 3: Best pharmacophore model AADR1 aligned with molecule 9. Pharmacophore features are color coded: hydrogen bond acceptor (A1, A2; pink), hydrogen bond donor (D7; blue) and aromatic ring (R9; orange).

Then fitness scores for all ligands were observed on the best scored pharmacophore model AADR1. The greater the fitness score, the greater the activity prediction of the compound. The fit function does not only check if the feature is mapped or not, it also contains a distance term, which measures the distance that separates the feature on the molecule from the centroid of the hypothesis feature. Table 4 shows the fitness score for all the molecules of training set. Figure 3 shows the AADR1 aligned with ligand having maximum fitness score, i.e. molecule 9 (IC_{50} = 75µm) of the training set.

Beside this survival score analysis, another validation method to characterize the quality of AADR1 is represented by its capacity for correct activity prediction of training set molecules. AADR1 was regressed against the training set compound. Table 4 shows the actual and estimated inhibitory activities of the 21 molecules from the training set based on the pharmacophore hypothesis AADR1. The predicted α-glucosidase inhibitory activity of training set molecule exhibited a correlation of 0.903 with reported α -glucosidase inhibitory activity using model AADR1 (Figure 4).

Table 4: Experimental and predicted IC_{50} values of training set molecules based on hypothesis AADR1

Comp. No.	Experimental IC_{50} (µM)	Predicted IC_{50} (µM)	Fitness Score	Comp. No.	Experimental IC_{50} (µM)	Predicted IC_{50} (µM)	Fitness Score
1	12	94.75	2.80	12	201	240.41	1.63
2	501	414	2.52	13	75	116.94	1.74
3	301	387	2.51	14	2	13.77	1.66
4	21	53.08	2.81	15	4	-16.43	1.45
5	201	138.81	2.78	16	501	497.07	2.33
6	201	95.74	2.80	17	68	31.18	1.23
7	7	-5.88	2.75	18	37	22.30	2.46
8	12	20.41	2.78	19	179	172.54	1.35
9	75	69.40	3.00	20	57	71.11	2.18
10	14	40.45	1.44	21	185	179.30	1.35
11	7	24.53	2.46				

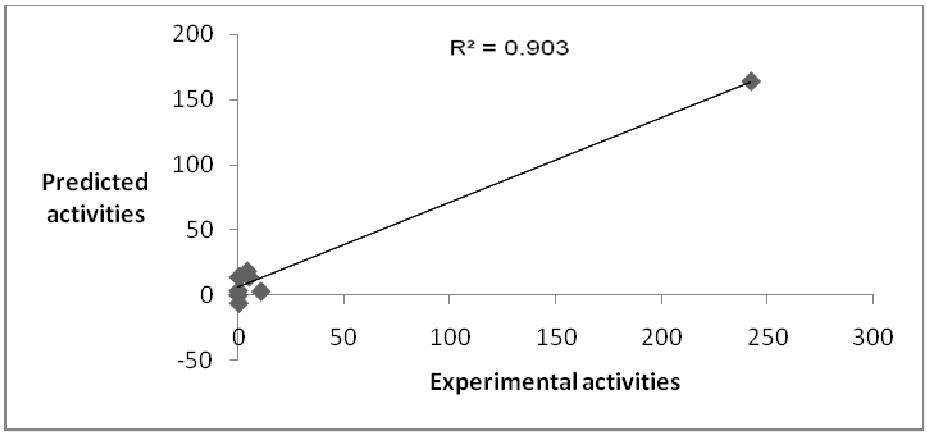

Figure 4: Relation between experimental and predicted α-glucosidase inhibitory activity values of training set molecules using model AADR1.

The validity and predictive character of AADR1 were further assessed by using the test set prediction. The test set having eight molecules was analyzed. All the test set molecules were built and minimized as well as used in conformational analysis like all training set molecules. Then the activities of test set molecules were predicted using AADR1 and compared with the actual activity. Actual and predicted activity values of test set molecules are given in Table 5. The predicted α-glucosidase inhibitory activity of test molecule exhibited a correlation of 0.69 with reported α -glucosidase inhibitory activity using model AADR1 (Figure 6). For a reliable model, the squared predictive correlation coefficient should be >0.60 [30, 31]. The results of this study reveal that model AADR1 can be used for the prediction of α-glucosidase inhibitory activity.

Table 5: Experimental and predicted IC_{50} values of test set molecules based on hypothesis AADR1

Comp. No	Experimental IC_{50} (μM)	Predicted IC_{50} (μM)	Fitness Score	Comp. No.	Experimental IC_{50} (μM)	Predicted IC_{50} (μM)	Fitness Score
1	5	15.65	2.72	5	501	306.36	2.35
2	13	102.37	1.50	6	45	79.44	2.42
3	150	100.69	2.65	7	150	124.71	1.21
4	201	152.61	1.54	8	358	106.85	1.27

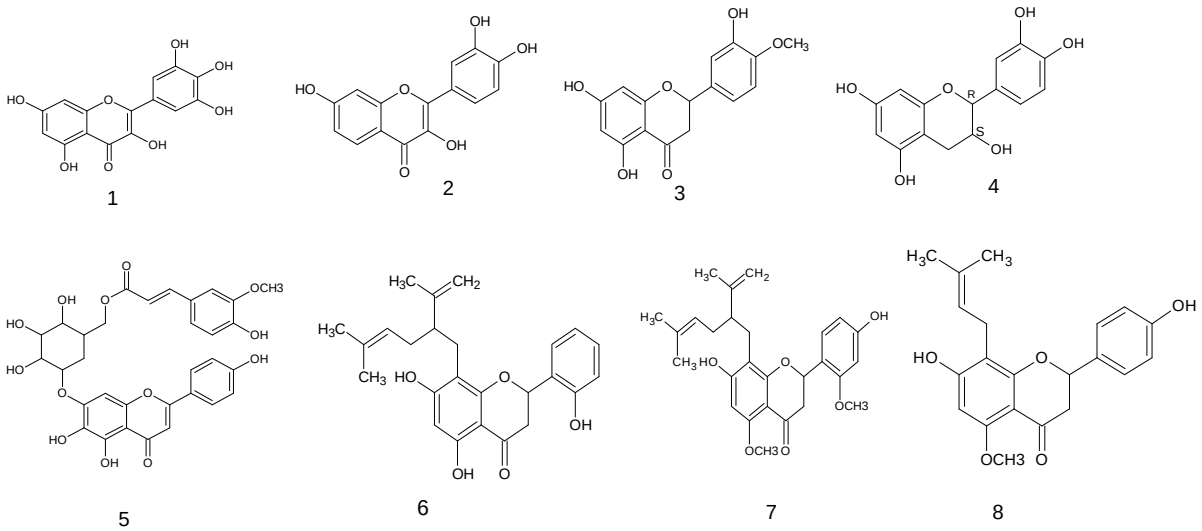

Figure 5: Chemical structures of the 8 test set molecules

3-D QSAR analysis

Additional insight into the α-glucosidase inhibitory activity can be gained by visualizing the 3-D QSAR model in the context of one or more ligands in the series with varying activity. This information can then be used to design new or more active analogues. 3-D QSAR models based on the molecules of training and test set using various features, i.e., hydrogen bond donor, hydrogen bond acceptors and aromatic ring has been studied.

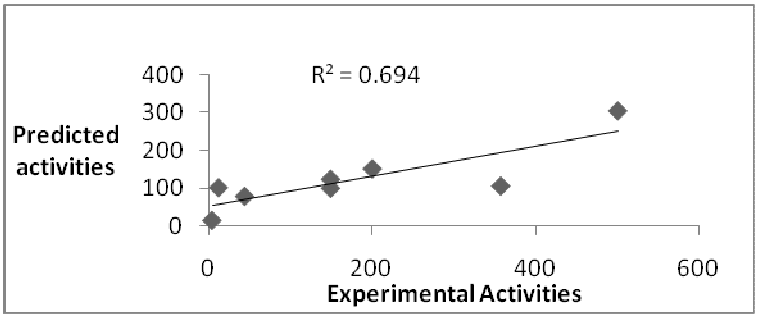

Figure 6: Relation between experimental and predicted α-glucosidase inhibitory activity values of test set molecules using model AADR1.

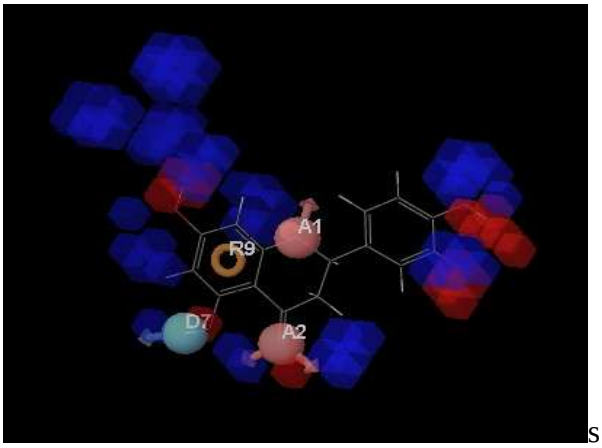

s

Figure 7: 3-D QSAR model based on molecule 9 of training set illustrating hydrogen bond donor feature

Hydrogen bond donor field predictions: The 3-D QSAR model based on molecule 9 of the training set using hydrogen bond donor feature is shown in Figure 7. Blue region near and around the ortho and meta hydrogen of phenyl ring substituted at position 2; hydrogen of OH group at position 5; and hydrogens at position 6, 8 of benzopyran indicates that the substitutions at these positions by groups having more hydrogen bond donor property favours the α-glucosidase inhibitory activity. Red region around the OH group at para position of phenyl ring, oxygen of carbonyl group at position 4, oxygen of OH at position 5 and oxygen of OH at position 7 of benzopyran indicates that substitutions at these positions by groups having hydrogen bond donor property do not favors α-glucosidase inhibitory activity.

Hydrogen bond acceptor field prediction: The 3-D QSAR model based on molecule 9 of the training set using hydrogen bond acceptor feature is shown in Figure 8. Blue region around oxygen at position 1, oxygen of carbonyl group at position 4, oxygen of OH at position 5 and oxygen of OH group at position 7 of benzopyran indicates that the substitutions at these positions by groups having more hydrogen bond acceptor property favours the α-glucosidase inhibitory activity. Red region around the para OH group of phenyl ring at position 2 of benzopyran do not favor the α-glucosidase inhibitory activity. Replacement of this OH group by any electron withdrawing group such as NO_2, OCH_3, Cl. F, Br etc. will result in increase in α-glucosidase inhibitory activity.

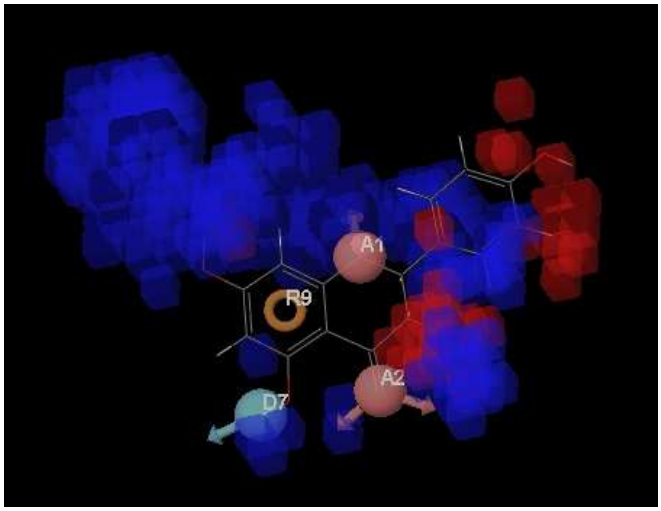

Figure 8: 3-D QSAR model based on molecule 9 of training set illustrating hydrogen bond acceptor feature

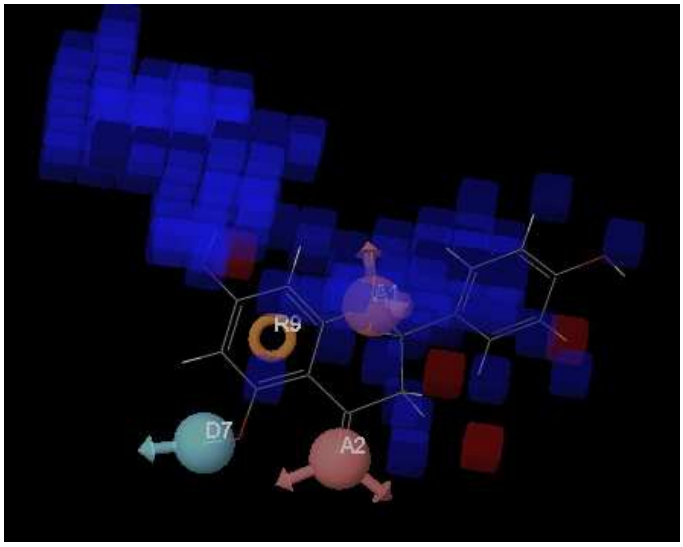

Figure 9: 3-D QSAR model based on molecule 9 of training set illustrating hydrophobic feature.

Hydrophobicity field prediction: The 3-D QSAR model based on molecule 9 of the training set using hydrophobicity feature is shown in Figure 9. Blue region around hydrogens at position 3, and position 8, ortho hydrogen of phenyl ring at position 2 and hydrogen of OH at para position of phenyl ring favours α-glucosidase inhibitory activity and substitutions at these positions by more hydrophobic groups will result in increase in α-glucosidase inhibitory activity. This is inconsistent with the observation that the replacement of hydrogen at position 3 of benzopyran by gallat results in increase in α-glucosidase inhibitory activity e.g. molecule 14 of training set having gallat at position 3 of benzopyran is more active (IC_{50} = 2 μM) as compared to the molecule 9 (IC_{50} = 75 μM) of training set. Similarly, replacement of hydrogen at position 8 of benzopyran by more hydrophobic groups result in good α-glucosidase inhibitory activity as exemplified by the observation that molecule 6 of test set (IC_{50} = 45 μM) and molecule 17, 18 of training set (IC_{50} = 68, 37 μM respectively) having alkene group at position 8 of benzopyran are more active as compared to the molecule 9 (IC_{50} = 75 μM) of training set.

CONCLUSION

The study shows the generation of a pharmacophore model AADR1 for flavonoids acting as α-glucosidase inhibitors. Pharmacophore modeling correlates activities with the spatial arrangement of various chemical features. Hypothesis AADR1 represents the best pharmacophore model for determining α-glucosidase inhibitory activity. AADR1 consists of two hydrogen bond acceptor, one hydrogen bond donor, and one aromatic ring features. This pharmacophore model was able to accurately predict α-glucosidase inhibitory activity and the validation results also provide additional confidence in the proposed pharmacophore model. Results suggested that the proposed 3-D QSAR model can be useful to rationally design new flavonoid molecules as α-glucosidase inhibitors and also to identify new promising molecules as α-glucosidase inhibitors in large 3-D database of molecules.

REFERENCES

[1] G. M. Reaven, *Diabetes*, **1988**, 37, 1595-1607.
[2] P. Z. Zimmet, K. G. Albert, J. Shaw, *Nature*, **2001**,414, 782-787.
[3] S. E. Inzucchi, *J. Am. Med. Assoc.*, **2007**, 287, 360-372.
[4] D. E. DeWitt, I. B. Hirsch., *J. Am. Med. Assoc.*, **2003**, 289, 2254-2264.
[5] D. E. DeWitt, D. C. Dgdale, *J. Am. Med. Assoc*, **2003**, 289, 2265-2269.
[6] H. E. Lebovitz, *Diabetes Rev*, **1999**, 7, 139-153.
[7] K. Cusi, R. A. DeFronzo, *Diabetes Rev*, **1998**, 6, 89-131.
[8] M. Diamant, R. J. Heine, *Drugs*, **2003**, 63, 1373-1405.
[9] H. E. Lebovitz, *Diabetes Rev*, **1998**, 6, 132-145.
[10] A. Ceriello, *Diabetes*, **2005**, 54, 1–7.
[11] Ujma saqib, Mohammadh Imran Siddiqi, *International journal of integrative biology*, **2008**, 2, 115-121.
[12] J. L. Chiasson, R. G. Josse, R. Gomis, *Lancet*, **2002**, 359, 2072–7.
[13] S. Yamagishi, T. Matsui, S. Ueda, K. Fukami, S. Okuda, *Curr Drug Metab.*, **2009**, 10, 159–163.
[14] C. A. Sotriffer, R. H. Winger, K. R. Liedl, Rode, M. Bernd, J. M. Varga, *Journal of Computer-Aided Molecular Design*, **1996**, 1, 305-320.
[15] S. S. Narkhede, M. S. Degani, *QSAR Comb Sci.* **2007**, 26, 744–753.
[16] S. Vepuri, N.R. Tawari, M. S. Degani, *QSAR Comb Sci.* **2007**, 26, 204–214.
[17] S. Ramar, S. Bag, N. R.Tawari, M. S. Degani, *QSAR Comb Sci.*, **2007**, 26, 608- 617.
[18] V. Hariprasad, V.M. Kulkarni, *J. Comp. Aided Mol. Des.*, **1996**, 10, 284.
[19] T. Kenjiro, M. Yuji, T. Kauta, M. Tomoko. *J. Nutr. Sci. Vitaminol*, **2006**, 52, 149-153.
[20] PHASES, Version 3.0, Schrödinger, LLC, NY**2008.**
[21] Maestro, Version 8.5, Schrödinger, LLC, NY**2008**.
[22] W. C. Still, A. Tempczyk, R. C. Hawley, T. Hendrickson, *J. Am. Chem. Soc.*, **1990**, 112, 6127.
[23] N. R. Tawari, Bag Seema, Mariam, S. Degani, *J. Mol. Model.* 14(10) (**2008**); 911–921.
[24] D. B. Boyd, Successes of computer-assisted molecular design, in: *Reviews in computational chemistry*, VCH, New York, **1990**, 4, 355–371.
[25] H.E. Lebovitz, *Endocrinology and Metabolism Clinics*, **1997**, 26, (3), 539–551.
[26] F. A. Van de Laar, P.L. Lucassen, , R. P. Akkermans, E. H. Van de Lisdonk, G.E. Rutten, C. Van Weel, *Cochrane Database of Systematic Reviews*, **2005**, 18 (2), pCD003639.
[27] H. Bischoff, W. Puls, H. P. Karause, H. Schutt, G. Thomas, *Diabetes Research and Clinical Practice*, **1985**, 1, 53- 62.

[28] S. H. Lam, J. M. Chen, C.J. Kang, C. H. Chen, S.H. Lee, *Phytochemisty*, **2008**, 69, 5, 1173-1178.
[29] Guner, F. Osman, *Pharmacophore perception***,** ISBN 0-9636817-6-1.
[30] H. Dureja, V. Kumar, S. Gupta, A. K**.** Madan, *J. Theo. Comput. Chem.*, **2007**, 6(3), 435–448.
[31] S. Wold, *Quant. Struct. Act. Relat.*, **1991**, 10**,** 191-193.